Applied Physics Letters

Band alignment at β-Ga_2O_3/III-N (III = Al, Ga) interfaces through hybrid functional calculations

Cite as: Appl. Phys. Lett. **117**, 102103 (2020); https://doi.org/10.1063/5.0020442
Submitted: 30 June 2020 . Accepted: 27 August 2020 . Published Online: 08 September 2020

Sai Lyu, and Alfredo Pasquarello

Applied Physics Letters ARTICLE scitation.org/journal/apl

Band alignment at β-Ga_2O_3/III-N (III = Al, Ga) interfaces through hybrid functional calculations

Cite as: Appl. Phys. Lett. **117**, 102103 (2020); doi: 10.1063/5.0020442
Submitted: 30 June 2020 · Accepted: 27 August 2020 ·
Published Online: 8 September 2020

Sai Lyu[a] and Alfredo Pasquarello

AFFILIATIONS

Chaire de Simulation à l'Echelle Atomique (CSEA), Ecole Polytechnique Fédérale de Lausanne (EPFL), CH-1015 Lausanne, Switzerland

Note: This paper is part of the Special Topic on Ultrawide Bandgap Semiconductors.
[a]**Author to whom correspondence should be addressed:** sai.lyu@epfl.ch

ABSTRACT

The band alignment and the chemical bonding at the β-Ga_2O_3/AlN and β-Ga_2O_3/GaN interfaces are studied through hybrid functional calculations. We construct realistic slab models with III–O (III = Al, Ga) bonds dominating the chemical bonding at both interfaces. The epitaxial relationships between β-Ga_2O_3 and wurtzite AlN and GaN determined from experiments are adopted in our slab models. These models satisfy electron counting rules, and all the dangling bonds are saturated at the interfaces. β-Ga_2O_3 is found to form type II heterojunctions with both wurtzite AlN and GaN. For the interfaces with AlN and GaN substrates, the calculated valence band offsets are 0.74 and 0.90 eV, respectively. These are in good agreement with the experimental values. The obtained band alignments are useful for designing optical and electronic devices based on β-Ga_2O_3 and group III nitrides.

β-Ga_2O_3 has attracted a great deal of attention because of its promising applications particularly in high-power electronics.[1,2] This material has a remarkable high breakdown electric field exceeding that of the widely used SiC and GaN.[1,2] Its wide bandgap of 4.5–4.9 eV makes it also suitable for fabricating solar-blind ultraviolet (UV) photodetectors.[3,4] Most importantly, single-crystal wafers can be obtained at low cost from the melt.[5] Moreover, the possibility of alloying this oxide with Al_2O_3 to form β-$(Al_xGa_{1-x})_2O_3$[6,7] provides high flexibility for bandgap engineering and device design. Group-III nitrides have been intensively studied because of their wide applications in optoelectronic and power devices.[8] The advantages of using III-N and their alloys are their tunable bandgaps and chemical stability. The in-plane lattice mismatch between the $(\bar{2}01)$ plane of β-Ga_2O_3 and the (0001) plane of wurtzite AlN and GaN is small so that high-quality epitaxial growth can be easily achieved,[9] which is helpful to minimize interfacial defects. The (0001) plane cut for III-N leads to polar interfaces between β-Ga_2O_3 and III-N. Recently, the heterojunctions between β-Ga_2O_3 and GaN or AlN have been experimentally studied by several groups.[9–13] These heterojunctions are expected to be used in ultraviolet photodetectors in which β-Ga_2O_3 is fabricated as a window material of UV light in view of its large bandgap and high thermal and chemical stabilities.[12] In addition, bipolar devices based on these heterojunctions are appealing because efficient p-type AlN or GaN and n-type Ga_2O_3 have already been achieved.[14] The construction of bipolar devices overcomes the problem of efficiently p-doping β-Ga_2O_3, which currently limits the potential of this material.[15]

Band offsets are key parameters in heterojunction device designs because they determine the transport properties. For the interfaces between β-Ga_2O_3 and wurtzite AlN or GaN, the reported band alignment can vary by as much as 1 eV.[9–12] Such an ambiguity also holds for some other dielectric materials deposited on β-Ga_2O_3.[16] Therefore, computational investigations are necessary to accurately determine the intrinsic band offsets of these interfaces.

In this work, we study the interface between β-Ga_2O_3 and III-N through first-principles calculations. We employ state-of-the-art hybrid functionals to overcome the bandgap problem of density functional theory (DFT). The accuracy of hybrid functionals in the calculation of band offsets has already been demonstrated and found to be on the order of ~0.2 eV,[17–24] conferring significant predictive capabilities to this method. The band offsets are derived by applying an alignment scheme in which interface calculations and bulk calculations of the interface components are combined. In the polar interface calculations, the in-plane strains due to the mismatch and the built-in electric fields due to the nonvanishing macroscopic polarization are also taken into account. We obtain valence band offsets (VBOs) of 0.74 and 0.90 eV for β-Ga_2O_3/AlN and β-Ga_2O_3/GaN interfaces, respectively.

The geometry optimization and electronic structure calculations are performed with the CP2K package.[25] Within the Gaussian plane wave (GPW) method, the DFT Kohn–Sham equations[26] are efficiently solved in a Gaussian-type basis set, while the electron density is expanded using an auxiliary plane wave (PW) basis set. We use double-ξ MOLOPT basis sets.[27] The valence–core interactions are described by Goedecker–Teter–Hutter (GTH)[28] pseudopotentials. For Ga, the 3*d* states are treated as valence states.[50] For the geometry optimizations, we use the semilocal generalized gradient approximation (GGA) proposed by Perdew–Burke–Ernzerhof (PBE).[29] For the electronic structure calculations of the bulk components, i.e., β-Ga_2O_3, AlN, and GaN, we use PBE0 (α) hybrid functionals[30,31] in which the fractions α of the Fock exchange are adjusted to reproduce the experimental bandgaps. It has been demonstrated that Koopmans' condition is closely satisfied for such hybrid functionals.[32] The PW energy cutoff is set to 600 Ry, and only the Γ point is sampled in the Brillouin zone as the supercells are sufficiently large to ensure convergence. In the PBE0 (α) calculations, an auxiliary basis set for the auxiliary density matrix method is employed to speed up the Fock exchange calculations.[33]

We determine the band alignment at the interface by using the method developed in Refs. 34 and 35, which is compatible with the presence of built-in electric fields. The VBO of a heterojunction *A*/*B* is expressed as

$$\mathrm{VBO}(A/B) = (E^B_{\mathrm{VBM}} - \bar{V}^B) - (E^A_{\mathrm{VBM}} - \bar{V}^A) + (\bar{V}^B - \bar{V}^A), \quad (1)$$

where $E_{\mathrm{VBM}} - \bar{V}$ is the energy difference between the valence band maximum (VBM) and the local reference level obtained in two separate bulk calculations for interface components *A* and *B*, and $\bar{V}^B - \bar{V}^A$ is the interface lineup term obtained in the interface calculation. The interface lineup is obtained at the PBE0(α) level, in which α is the average of the exchange mixing parameters pertaining to the two interface components.[17,19,23,36] The average electrostatic potential is chosen as the local reference level. The conduction band offset (CBO) between A and B can then be derived by using the bandgap E_g of each interface component,

$$\mathrm{CBO}(A/B) = (E^B_g - E^A_g) + \mathrm{VBO}(A/B). \quad (2)$$

Since the interface is perpendicular to the polar (0001) axis of wurtzite AlN or GaN, the macroscopic polarization in the nitride layers induces finite electric fields in the bulk components.[37] To deal with the finite bulk electric fields, we adopt the scheme proposed by Foster and Schneider.[38] We first apply a double convolution[39] over the planar average of the electrostatic potential $V(z)$ along the direction z, which is orthogonal to the interface plane. Then, we take the nominal interface position at the midway between the atomic planes that form the interface.[38] By extrapolating the macroscopically averaged electrostatic potential from each bulklike region to the nominal interface position, the interface lineup can be determined in a way that eliminates the effects of the electric fields.[38] The uncertainty in the interface lineup produced by the extrapolation procedure can be expressed as $|E_1 - E_2|\delta_z$,[38] where E_1 and E_2 are the electric fields in the bulklike regions of the two interface components, respectively, and δ_z is the uncertainty in the determination of the interface position. By setting δ_z to 25% of the atomic layer distance, we obtain a rough estimate of the errors involved in the potential lineups, which are found to not exceed 0.06 and 0.01 eV at β-Ga_2O_3/AlN and β-Ga_2O_3/GaN interfaces, respectively.

β-Ga_2O_3 shows a monoclinic crystal structure and has two types of coordinations for Ga^{3+} ions, pertaining to either distorted tetrahedra or distorted octahedra.[2,42] To determine the optimal fraction of Fock exchange to be used for β-Ga_2O_3, we use the experimental structure derived in Ref. 42 (see Table I). For bulk AlN and GaN, we perform full relaxations with the PBE functional. The obtained lattice parameters are given in Table I together with the corresponding experimental values. The bandgaps and VBM positions relative to the bulk averaged electrostatic potential of bulk β-Ga_2O_3, AlN, and GaN are obtained at the PBE0(α) level.

In experimental studies, the interfaces with β-Ga_2O_3 are usually grown by taking AlN or GaN as substrates.[9,11,12] In these lattice-mismatched cases, the substrate determines the in-plane lattice constants.[43] The biaxial strain caused by the lattice mismatch makes the β-Ga_2O_3 epilayer adopt a new interplane lattice constant. To model the β-Ga_2O_3/III-N (III = Al, Ga) interfaces, we follow the epitaxial relationships of β-Ga_2O_3 $(\bar{2}01) \parallel$ AlN (0001) and β-Ga_2O_3 [102] $\parallel$ AlN $[\bar{1}100]$, which have been determined experimentally.[9] The same epitaxial relationships are also applied to the GaN case. In order to minimize the interfacial lattice mismatch, we construct an orthorhombic 510-atom supercell containing a III-N (0001) slab with an (8×2) in-plane periodicity and a β-Ga_2O_3 $(\bar{2}01)$ slab with a (3×2) in-plane periodicity (cf. Figs. 1 and 2). The *x* and *y* axes correspond to the [102] and [010] crystal axes of β-Ga_2O_3, respectively. For AlN, this yields in-plane lattice mismatches of -1.4% and 3.0% along the *x* and *y* axes, respectively. In the case of GaN, the respective mismatches are 1.7% and 6.0%. In this way, β-Ga_2O_3 is strained and lattice matched to AlN

TABLE I. Lattice parameters, bandgaps (in eV), and VBM positions (in eV) relative to the bulk averaged electrostatic potential of β-Ga_2O_3, AlN, and GaN obtained at the PBE0(α) level. The lattice parameters of β-Ga_2O_3 are experimental values taken from Ref. 42 and correspond to the conventional unit cell.[40] The exchange mixing parameters α, which reproduce the experimental bandgaps for each material, are also given.

	a (Å)	b (Å)	c (Å)	β	α	E_g	VBM
β-Ga_2O_3	12.23	3.04	5.80	103.70°	0.27	4.87	2.99
	a (Å)		c (Å)	u	α	E_g	VBM
AlN	3.14		4.98	0.384	0.25	6.07	4.73
Expt.[41]	3.11		4.98	0.382			
GaN	3.24		5.24	0.377	0.27	3.37	4.46
Expt.[41]	3.19		5.19	0.377			

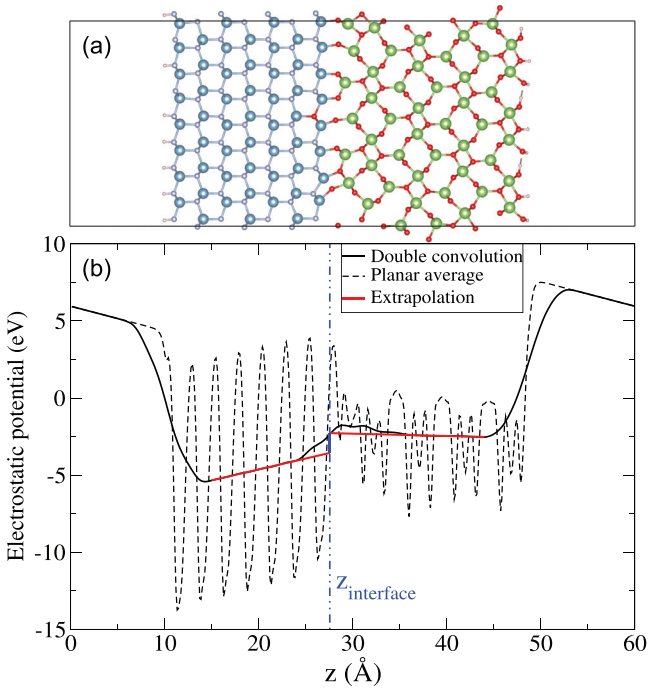

FIG. 1. (a) Atomistic model of the relaxed β-Ga_2O_3/AlN interface obtained at the PBE level and (b) its planar and macroscopically averaged electrostatic potential obtained at the PBE0(α) level. The interface lineup is determined to be 1.29 eV.

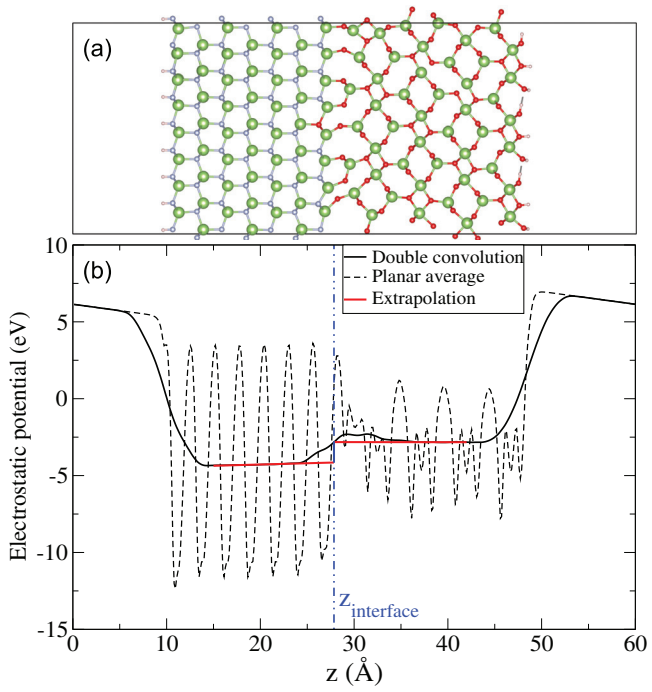

FIG. 2. (a) Atomistic model of the relaxed β-Ga_2O_3/GaN interface obtained at the PBE level and (b) its planar and macroscopically averaged electrostatic potential obtained at the PBE0(α) level. The interface lineup is determined to be 1.33 eV.

or GaN in the same way as in the experiments.[9,11,12] The z-axis coincides with the AlN [0001] direction, while the x and y axes are parallel to the $[\bar{1}100]$ and $[11\bar{2}0]$ directions of AlN, respectively. Since the x and y axes also match the [102] and [010] directions of β-Ga_2O_3, the periodicities are maintained along these two orthogonal directions in the interface supercell model. At the interface, III–O bonds are used to bridge the oxide slab to the AlN or GaN slab. III–O bonds are expected to be more stable than Ga–N bonds because of the higher electronegativity difference. Some interfacial O atoms are twofold coordinated and thus show a different coordination than in bonding configurations of the bulk. In bulk β-Ga_2O_3, oxygen atoms are either threefold or fourfold coordinated. However, the O atom admits flexible bonding patterns as it can transfer nonbonded electrons to lone pair states. It is interesting to note that each Ga layer parallel to the $(\bar{2}01)$ plane can only contain either fourfold or sixfold coordinated Ga atoms and these two types of Ga layers alternate along the direction perpendicular to the $(\bar{2}01)$ plane. In the interface model, a thick vacuum layer (~20 Å) is added to minimize image interactions due to the periodic boundary condition in the z direction.

We stress that our interface model satisfies the electron counting rule.[24,44–46] In this interface model, each cation layer in β-Ga_2O_3 slab contains 12 Ga^{3+} ions, while each anion layer contains 18 O^{2-} ions. We create two O vacancies at the interface where sixteen III–O bonds are formed and each surface group-III atom forms one III–O bond. The Ga atoms in the subsurface Ga layer of the oxide are all fourfold coordinated. The dangling bonds of the surface Ga atoms caused by the O vacancies are saturated by the adjacent O atoms. Therefore, no dangling bonds are present at the interface. The interfacial O layer has 16 O^{2-} ions, contributing with −32 charges. For this interfacial O layer, the subsurface Ga layer gives +18 charges and the surface III layer gives +12 charges, adding up to +30 charges. To provide the additional +2 charges, we replace two subsurface N sites by two substitutional O_N. In this way, the interface is charge neutral (insulating) and the electron counting rule is satisfied. Hydrogen atoms are used to passivate the bottom N layer and top O layer, so that the two surfaces are insulating without any gap states. After carrying out full structural relaxations of the atomic positions in the interface models, we use the procedures described above to determine the interface lineups. Our model interfaces with the extrapolated electric fields are illustrated in Figs. 1 and 2. The calculated potential lineups at the β-Ga_2O_3/AlN and β-Ga_2O_3/GaN interfaces are 1.29 and 1.33 eV, respectively.

In order to account for the effect of strain on β-Ga_2O_3, we determine the equilibrium lattice parameters of β-Ga_2O_3 with the in-plane lattice constants controlled by the substrate and evaluate the corresponding bandgaps and VBM levels. To expose the $(\bar{2}01)$ surface of β-Ga_2O_3 as in the interface models, we transform the conventional unit cell into a larger monoclinic one in which the first lattice vector $\mathbf{a}'$ of the unit cell is transformed to $\mathbf{a} + 2\mathbf{c}$, while the other two remain the same and β' is the angle between $\mathbf{a}'$ and $\mathbf{c}$. This larger unit cell is strained to have the in-plane lattice constants (a' and b) determined by the AlN or GaN substrates and the other lattice parameters (c and β') as well as the atomic positions are optimized. The calculated bandgaps and VBM levels of β-Ga_2O_3 subject to different substrates are given in Table II. We use the same exchange mixing parameter $\alpha = 0.27$ as for the unstrained bulk. Here, we assume that the electrostatic potential levels of the strained orthorhombic β-Ga_2O_3 $(\bar{2}01)$ slab in the interface model and of strained monoclinic β-Ga_2O_3 are the

TABLE II. Lattice parameters, bandgaps (in eV), and VBM positions (in eV) relative to the bulk averaged electrostatic potential of strained β-Ga_2O_3 corresponding to different substrates.

Strained	Substrate	a' (Å)	b (Å)	c (Å)	β'	E_g	VBM
β-Ga_2O_3	AlN	14.48	3.14	6.08	52.2°	4.38	2.70
β-Ga_2O_3	GaN	14.94	3.24	6.08	50.5°	4.13	2.23

same. We validate this assumption by comparing the average electrostatic potential levels with respect to the vacuum level in strained orthorhombic and monoclinic β-Ga_2O_3 ($\bar{2}01$) slabs. Taking structures corresponding to the AlN substrate as an example, we obtained a difference of only 0.03 eV, which negligibly affects the alignment.

The calculated band offsets at the β-Ga_2O_3/III-N interfaces and the comparison with the available experimental results are given in Table III. In Fig. 3, we schematically show the calculated band offsets. β-Ga_2O_3 forms type II heterojunctions with both AlN and GaN.

For β-Ga_2O_3 grown on an AlN substrate, the calculated VBO of 0.74 eV is in good agreement with the value of 0.55 eV reported by Sun *et al.*[9] We suggest that this good agreement stems from the fact that the same epitaxial relationships are used in the model and in the experiment. This minimizes defect generation at the interface, and the measured offset thus remains close to its intrinsic value, which corresponds to the target of our calculations.

Additionally, to compare with the recent experimental data of Chen *et al.*,[10] we also consider AlN grown on a β-Ga_2O_3 substrate. In this case, we obtain a VBO of 0.56 eV and a CBO of 1.90 eV. Hence, the VBO is found to decrease by 0.18 eV with respect to that of β-Ga_2O_3 grown on an AlN substrate (cf. Table III). The major part (0.10 eV) of this decrease results from the shifts of the bulk bands in response to strain (deformation potential theory), as we checked by obtaining the VBM levels in unstrained and strained bulk materials with respect to the vacuum level. However, despite the use of the same strain conditions as in the experiment, our calculated VBO of 0.56 eV differs noticeably from the measured values of 0.09 and −0.72 eV, which refer to two different preparation methods.[10] Since the difference largely exceeds the accuracy of ∼0.2 eV expected from this type of hybrid functional calculations,[17–20] we conclude that the observed discrepancies do not depend on strain but rather arise from the departure from the nearly abrupt epitaxial interface modeled in our setup.

TABLE III. Calculated band alignment at β-Ga_2O_3/III-N interfaces and comparison with the available experimental results. Energies are given in units of eV.

Interface	VBO	CBO	References	Substrate
β-Ga_2O_3/AlN	0.74	2.43	Present	AlN
	0.55		Ref. 9	AlN
	0.56	1.90	Present	β-Ga_2O_3
	0.09		Ref. 10	β-Ga_2O_3
	−0.72		Ref. 10	β-Ga_2O_3
β-Ga_2O_3/GaN	0.90	0.14	Present	GaN
	0.78		Ref. 12	GaN
	1.40		Ref. 11	GaN

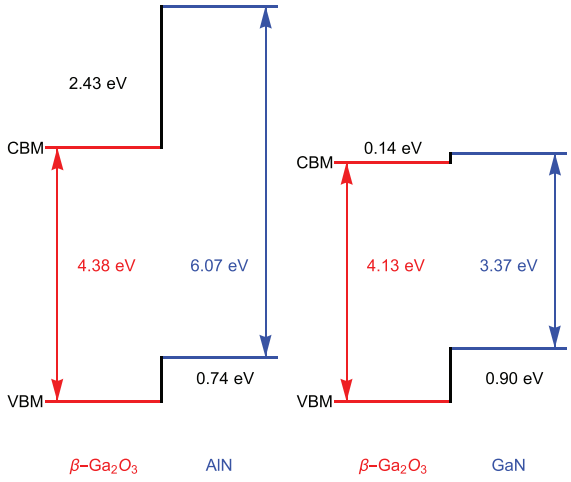

FIG. 3. The band alignment diagrams of the β-Ga_2O_3/AlN and β-Ga_2O_3/GaN heterojunctions.

For β-Ga_2O_3 grown on a GaN substrate, the calculated VBO of 0.90 eV falls well within the experimental range of 0.78–1.40 eV. The experimental results are obtained through x-ray photoemission spectroscopy (XPS) and thus might suffer from inaccuracies due to the averaging over a spatial layer subject to built-in electric fields. The difference in VBOs between β-Ga_2O_3/AlN and β-Ga_2O_3/GaN is consistent with the trend in the electron affinities of AlN and GaN.[47,48]

In conclusion, we studied the band offsets and the chemical bonding at β-Ga_2O_3/AlN and β-Ga_2O_3/GaN interfaces through advanced electronic-structure calculations. The obtained band offsets are consistent with the experimental values and provide accurate estimates for the intrinsic values pertaining to nearly abrupt epitaxial interfaces. The present study introduces modeling procedures that can straightforwardly be applied to β-Ga_2O_3/$Al_xGa_{1-x}N$ interfaces, which are considered in UV detectors or light emitting diodes.[9] More generally, this study shows how to deal with band alignments involving the ($\bar{2}01$) interface of β-Ga_2O_3. These band alignments are important for the design of devices based on β-Ga_2O_3.

This work has benefited from partial support within the context of the National Center of Competence in Research (NCCR) "Materials' Revolution: Computational Design and Discovery of Novel Materials (MARVEL)" of the SNSF. The calculations have been performed at the Swiss National Supercomputing Centre (CSCS) (grant under Project ID s879) and at SCITAS-EPFL.

DATA AVAILABILITY

The data that support the findings of this study are openly available in the Materials Cloud platform at https://doi.org/10.24435/materialscloud:g5-9z, Ref. 49.

REFERENCES

[1]M. Higashiwaki, K. Sasaki, A. Kuramata, T. Masui, and S. Yamakoshi, Appl. Phys. Lett. **100**, 013504 (2012).
[2]M. A. Mastro, A. Kuramata, J. Calkins, J. Kim, F. Ren, and S. J. Pearton, ECS J. Solid State Sci. Technol. **6**, P356 (2017).

[3]A. M. Armstrong, M. H. Crawford, A. Jayawardena, A. Ahyi, and S. Dhar, J. Appl. Phys. **119**, 103102 (2016).
[4]J. Kim, S. Oh, M. A. Mastro, and J. Kim, Phys. Chem. Chem. Phys. **18**, 15760 (2016).
[5]A. Kuramata, K. Koshi, S. Watanabe, Y. Yamaoka, T. Masui, and S. Yamakoshi, Jpn. J. Appl. Phys., Part 1 **55**, 1202A2 (2016).
[6]T. Wang, W. Li, C. Ni, and A. Janotti, Phys. Rev. Appl. **10**, 011003 (2018).
[7]A. Ratnaparkhe and W. R. L. Lambrecht, Phys. Status Solidi B **257**, 1900317 (2020).
[8]T. D. Moustakas and R. Paiella, Rep. Prog. Phys. **80**, 106501 (2017).
[9]H. Sun, C. G. T. Castanedo, K. Liu, K.-H. Li, W. Guo, R. Lin, X. Liu, J. Li, and X. Li, Appl. Phys. Lett. **111**, 162105 (2017).
[10]J.-X. Chen, J.-J. Tao, H.-P. Ma, H. Zhang, J.-J. Feng, W.-J. Liu, C. Xia, H.-L. Lu, and D. W. Zhang, Appl. Phys. Lett. **112**, 261602 (2018).
[11]W. Wei, Z. Qin, S. Fan, Z. Li, K. Shi, Q. Zhu, and G. Zhang, Nanoscale Res. Lett. **7**, 562 (2012).
[12]P. Li, H. Shi, K. Chen, D. Guo, W. Cui, Y. Zhi, S. Wang, Z. Wu, Z. Chen, and W. Tang, J. Mater. Chem. C **5**, 10562 (2017).
[13]A. Kalra, S. Vura, S. Rathkanthiwar, R. Muralidharan, S. Raghavan, and D. N. Nath, Appl. Phys. Express **11**, 064101 (2018).
[14]J. Montes, C. Yang, H. Fu, T.-H. Yang, K. Fu, H. Chen, J. Zhou, X. Huang, and Y. Zhao, Appl. Phys. Lett. **114**, 162103 (2019).
[15]A. Kyrtsos, M. Matsubara, and E. Bellotti, Appl. Phys. Lett. **112**, 032108 (2018).
[16]S. J. Pearton, J. Yang, P. H. Cary, F. Ren, J. Kim, M. J. Tadjer, and M. A. Mastro, Appl. Phys. Rev. **5**, 011301 (2018).
[17]A. Alkauskas, P. Broqvist, F. Devynck, and A. Pasquarello, Phys. Rev. Lett. **101**, 106802 (2008).
[18]P. Broqvist, J. F. Binder, and A. Pasquarello, Appl. Phys. Lett. **94**, 141911 (2009).
[19]K. Steiner, W. Chen, and A. Pasquarello, Phys. Rev. B **89**, 205309 (2014).
[20]D. Colleoni, G. Miceli, and A. Pasquarello, Appl. Phys. Lett. **107**, 211601 (2015).
[21]Y. Hinuma, Y. Kumagai, I. Tanaka, and F. Oba, Phys. Rev. B **95**, 075302 (2017).
[22]T. Wang, C. Ni, and A. Janotti, Phys. Rev. B **95**, 205205 (2017).
[23]L. Weston, H. Tailor, K. Krishnaswamy, L. Bjaalie, and C. G. Van de Walle, Comput. Mater. Sci. **151**, 174 (2018).
[24]Z. Zhang, Y. Guo, and J. Robertson, Appl. Phys. Lett. **114**, 161601 (2019).
[25]J. VandeVondele, M. Krack, F. Mohamed, M. Parrinello, T. Chassaing, and J. Hutter, Comput. Phys. Commun. **167**, 103 (2005).
[26]W. Kohn and L. J. Sham, Phys. Rev. **140**, A1133 (1965).
[27]J. VandeVondele and J. Hutter, J. Chem. Phys. **127**, 114105 (2007).
[28]S. Goedecker, M. Teter, and J. Hutter, Phys. Rev. B **54**, 1703 (1996).
[29]J. P. Perdew, K. Burke, and M. Ernzerhof, Phys. Rev. Lett. **77**, 3865 (1996).
[30]J. P. Perdew, M. Ernzerhof, and K. Burke, J. Chem. Phys. **105**, 9982 (1996).
[31]C. Adamo and V. Barone, J. Chem. Phys. **110**, 6158 (1999).
[32]G. Miceli, W. Chen, I. Reshetnyak, and A. Pasquarello, Phys. Rev. B **97**, 121112 (2018).
[33]M. Guidon, J. Hutter, and J. VandeVondele, J. Chem. Theory Comput. **6**, 2348 (2010).
[34]C. G. Van de Walle and R. M. Martin, Phys. Rev. B **34**, 5621 (1986).
[35]A. Baldereschi, S. Baroni, and R. Resta, Phys. Rev. Lett. **61**, 734 (1988).
[36]R. Shaltaf, G.-M. Rignanese, X. Gonze, F. Giustino, and A. Pasquarello, Phys. Rev. Lett. **100**, 186401 (2008).
[37]F. Bernardini and V. Fiorentini, Phys. Rev. B **57**, R9427–R9430 (1998).
[38]D. H. Foster and G. Schneider, "Band alignment and directional stability in abrupt and polar-compensated Si/ZnS interface calculations," arXiv:1403.5230 (2014).
[39]S. Baroni, R. Resta, A. Baldereschi, and M. Peressi, *NATO ASI Series* (Springer US, 1989), pp. 251–271.
[40]H. Peelaers and C. G. Van de Walle, Phys. Status Solidi B **252**, 828 (2015).
[41]H. Schulz and K. Thiemann, Solid State Commun. **23**, 815 (1977).
[42]S. Geller, J. Chem. Phys. **33**, 676 (1960).
[43]N. Tit, M. Peressi, and S. Baroni, Phys. Rev. B **48**, 17607 (1993).
[44]P. W. Peacock and J. Robertson, Phys. Rev. Lett. **92**, 057601 (2004).
[45]J. Robertson and L. Lin, Appl. Phys. Lett. **99**, 222906 (2011).
[46]L. Lin and J. Robertson, Appl. Phys. Lett. **98**, 082903 (2011).
[47]S. Lyu and W. R. L. Lambrecht, J. Phys. D **53**, 015111 (2020).
[48]P. G. Moses, M. Miao, Q. Yan, and C. G. Van de Walle, J. Chem. Phys. **134**, 084703 (2011).
[49]S. Lyu and A. Pasquarello (2020). "Band alignment at β-Ga2O3/III-N (III = Al, Ga) interfaces through hybrid functional calculations," Material Cloud Archive https://doi.org/10.24435/materialscloud:g5-9z
[50]A. Bouzid and A. Pasquarello, Phys. Status Solidi **13**, 1800633 (2019).